ANL/IPNS/CP-93090
CONF-970814--

July 14, 1997 version

Structure and Dynamics of Phosphate Glasses: from Ultra- to Orthophosphate Composition*

C.-K. Loong[1], K. Suzuya[2], D. L. Price[1], B. C. Sales[3], and L. A. Boatner[3]

[1]Argonne National Laboratory, Argonne, Illinois 60439-4814 U.S.A.

[2]JAERI, Kamigori, Ako, Hyogo 678-22, Japan

[3]Oak Ridge National Laboratory, Oak Ridge, TN 37831-6056 U.S.A.

Abstract

The short- and intermediate-range order as well as atomic dynamics in various phosphate glasses were investigated using neutron diffraction and inelastic scattering. The 3-D network of corner-sharing PO_4 tetrahedra in g-P_2O_5 is highly unstable and hygroscopic. Depolymerization of the network to chain-like structure and eventually to unconnected PO_4 units by incorporating alkali, alkali-earth or transition-metal modifiers is clearly evident in the structure factor S(Q) in the $Q < 4$ Å^{-1} region. The dynamic response to such structural changes is equally strong: e. g., the broad P-O stretching band extending to 170 meV in g-P_2O_5 is sharpened and shifted down to ~125 meV in the orthophosphate composition. The correlation between the microscopic structure and physical properties for a series of P-glasses is discussed.

Keywords: phosphate glasses, inorganic polymer, intermediate-range ordering, extended-range ordering

*An invited paper

Corresponding author: Chun Loong, IPNS, Bldg 360, Argonne National Laboratory, Argonne, IL 60439 USA.
Phone: 630-252-5596, FAX 630-252-4163, E-mail: ckloong@anl.gov

DISCLAIMER

1. Introduction

In glassy and crystalline phosphates the basic building blocks are PO_4 tetrahedra. sp^3 hybridization of the P outer electronic orbitals $(3s^2)(3p^3)$ gives rise to the directional σ-bonding between the P and O in a PO_4 unit. The remaining electron of P is promoted to 3d orbital, resulting in a $d\pi$-$p\pi$ bonding between P and O. In pure P_2O_5 the PO_4 tetrahedra are connected by sharing up to three oxygen atoms (bridging O) to form a 3-D network. The π-character associated with the P=O (nonbridging O) double bond is energetically unbalanced and there is a strong tendency to break up the cross-linking network. Pure g- or c-P_2O_5 are extremely hygroscopic and volatile. By incorporating counter cations (network modifier such as H, alkali, alkali-earth or transition metals) to create additional nonbridging O quickly improves the stability. The principal connectivity of the PO_4 tetrahedra transforms from 3-D networking (ultra-) to chain-like (meta-) to dimer-like (pyro-) to isolated (ortho-) configuration. Bulk ultra-, meta-, and pyrophosphate glasses containing a great variety of metal actions can be prepared by melt quenching or sol-gel processing methods.

The influence of the oxidation states, ionic sizes, electronic and magnetic properties of the metal cations on the chemical and structural properties of phosphate glasses is enormous. In additional to modification of the polymeric structure of the PO_4 chains, the metal cations may promote and/or activate certain reactions such as nucleation of crystalline grains or luminescence. These complex phenomena imply numerous opportunities in development of novel materials and devices for technological applications provided an understanding of the systematics and physical origins of such behavior is established so as to guide the development efforts. In fact, industrial investments in phosphate glasses as compared to the silicate

analogue have been limited due to the concerns of cost and chemical instability of the parent materials. Only until recently the technological importance of phosphate glasses and glass-ceramics is recognized.[1-25] Table 1 lists some areas of interests and potential applications of phosphate glasses. The advancement of the field is in part due to the availability of better experimental methods for characterization such as the high-performance liquid chromatography.[26] Neutron scattering permits the measurements of the static and dynamic structure factors from which important information regarding the structure and dynamics of a glassy or crystalline systems can be obtained. Here we report recent neutron studies of glassy $Na_2O{\bullet}P_2O_5$, $PbO{\bullet}P_2O_5$ systems over the ultra- to pyro-composition range and a Pb-Sc-P-O glass. We aimed at a characterization of the short-, intermediate-, and extended-range order structures as the composition changes from ultra- to pyrophosphate. The Pb-Sc-P-O glass features many desirable optical properties and the present study reveals the short-to-intermediate range order structure of Sc-O correlation.

2. Experimental

Anhydrous $(Na_2O)_x(P_2O_5)_{100-x}$ [x = 0, 10, 20 (ultraphosphates); and x = 50 (metaphosphate)] glasses were prepared at Argonne National Laboratory using procedures described elsewhere.[27] Results of chemical analysis of Na and P by atomic absorption spectrochemical and ICP emission spectrophotometric methods showed that the batched composition was retained within an uncertainty of 1 mol% after melting. The $(PbO)_y(P_2O_5)_{100-y}$ [y = 50 (metaphosphate) and 66.7 (pyrophosphate)], and $(PbO)_{54.2}(Sc_2O_3)_{3.6}(P_2O_5)_{42.2}$ glasses were prepared at Oak Ridge National Laboratory using methods described previously.[6, 28] The neutron time-of-flight diffraction and inelastic

experiments were carried out using the Glass, Liquid and Amorphous Diffractometer (GLAD) and the High- and Low-Resolution Medium-Energy Chopper Spectrometers (HRMECS and LRMECS) at the Intense Pulsed Neutron Source (IPNS) of Argonne National Laboratory. The capabilities and operation of these instruments have been described in detail previously[29, 30] so they are not repeated here. To assist data interpretation, we also performed neutron measurements on a $(PbO)_{56.2}(P_2O_5)_{43.8}$ glass (prepared at Argonne) and a $Pb_2P_2O_7$ polycrystalline sample (prepared at Oak Ridge).

3. Results and Discussion

3.1 $(Na_2O)_x(P_2O_5)_{100-x}$ glasses

Fig. 1 shows the static structure factors S(Q) of g-$(Na_2O)_x(P_2O_5)_{100-x}$ (x = 0, 10, 20, 50) in the Q = 0-15 Å^{-1} region obtained from the GLAD measurements at room temperature. Data were collected up to a much higher Q value (~40 Å^{-1}). The S(Q) for x = 50 is in good agreement with those of Suzuki *et al.*[31] and Hoppe *et al.*[32] The pair correlation function G(r) was obtained from a Fourier transform of the data according to

$$G(r) = \frac{1}{2\pi^2 \rho_0} \int_0^\infty [S(Q) - 1] Q^2 \frac{\sin Qr}{Qr} dQ \,. \qquad (1)$$

where ρ_0 is the density. The approximate characteristic correlation lengths for short-range (SR, r < 2 Å), intermediate-range (MR, 2 < r < 6.3 Å), and extended-range (ER, r > 6.3 Å) order can be identified with Q > 3, 1 < Q < 3, and Q < 1 Å^{-1}, respectively. The almost identical S(Q) for Q beyond ~3.5 Å^{-1} in all compositions, as shown in Fig. 1, indicates that addition of the Na^+ modifier to g-P_2O_5 has little effect on the SR order. But drastic changes of

the MR structure can be seen from the replacement of the two peaks of g-P_2O_5 by a single peak for 20 mol% Na_2O glass at 1.60 $Å^{-1}$, which corresponds to a correlation length of 3.7 Å. This indicates that the MR order structure characteristic to that of a P_4O_{10} molecule in the g-P_2O_5 is broken down into smaller units by the modifier cations. As the composition of Na_2O changes from 20 to 50 mol%, the MR order peak shifts to higher Q, indicating further destruction of the PO_4 linkage. Furthermore, a new peak arises at 1.16 $Å^{-1}$ for the 50 mol% composition, implying an ER order on an length scale of 5.4 Å presumably due to the formation of PO_4 chain-like structure in the metaphosphate.

The above qualitative arguments have been reinforced using a model of Random Packing of Structural Units proposed previously by Moss and Price[33] where additional information concerning the arrangement of the P_4O_{10} molecule-like units in g-P_2O_5. We also carried out additional measurements on $(K_2O)_x(P_2O_5)_{100-x}$ ($0 \leq x \leq 50$) as well as on alkali metaphosphate glasses, MPO_3 (M = Li, Rb, and Cs). The overall results confirmed the major effect of the modifier on the transformation of 3-D network in ultraphosphates to polymeric structure of PO_4 chains in metaphosphates. Detailed discussion of the effects of the cation size and the corresponding change in the glass-transition temperature is given in a separation publication.[27]

We now discuss the results of inelastic-scattering measurements. The obtained dynamic structure factor S(Q, E) contains information regarding the atomic motions over a range of characteristic interparticle correlation lengths $L = 2\pi/Q$ and energies E (vibrational frequencies). In disorder systems only the magnitude of the wavevector **Q** is relevant. The frequency distribution function obtained by summing S(Q, E) over a wide range of Q can be

converted to a generalized phonon density of states (PDOS). The spectral functions obtained by Raman and infrared spectroscopy, on the other hand, are determined by the polarizability and electric dipole moments, respectively, induced by the atomic vibrations only at Q = 0. In case of crystalline materials, symmetry properties of the long-range crystal structure may impose further restrictions (selection rules) to the observable vibrational modes by the optical experiments.

Fig. 2 (a and b) displays the observed generalized PDOS of c-P_2O_5 and g-P2O5 obtained from the LRMECS measurements at 15 K. The PDOS of c-P_2O_5 shows three wide bands within 40-120 meV with some fine structure at 42.5, 52.1, 74.2, 99.2, 107.5 meV. At higher energies there are three sharp peaks at 128.8, 145.8 and 173 meV which may be assigned as the symmetric stretch (ν_a) and asymmetric stretch (ν_s) vibrations of the O-P-O bonds, and the stretch vibrations of the double bond ν(P=O), respectively. Phonons below 120 meV correspond to various O-P-O, P-O-P out-of-plane motions and framework vibrations. In g-P_2O_5 the features below ~120 meV are much broader, reflecting a distribution of locally distorted PO_4 tetrahedra in the glass. The ν_a(O-P-O) and ν_s(O-P-O) peaks merge into a single broad band centered around 140 meV, and the ν(P=O) peak shifts down slightly to 169.6 meV.

Fig. 2 (c and d) displays the observed generalized PDOS of the $(Na_2O)_x(P_2O_5)_{100-x}$ (x = 0, 20 and 50) glasses at 15 K. At the 20 mol% of Na_2O composition all the features in the PDOS broaden significantly. The ν(P=O) peak shifts down to 165.5 meV and the $\nu_{a,s}$(O-P-O) band become very wide showing some fine structure at 122, 131 and 144.5 meV. A large portion of the phonon density in the 80-110 meV region is removed to lower energies. These

changes indicate that the 3-D network made up by corner sharing PO_4 tetrahedra is broken up significantly by the addition of Na^+ modifier. A large portion of the P-O-P links between adjacent PO_4 units are interrupted by O-Na-O bonding, resulting in a new MR order. The exceedingly broad phonon bands reflect a broad distribution of P-O-P and O-Na-O coordination in the MR (a length scale of 2 - 6 Å). At the metaphosphate composition (Fig. 2d), the features in the PDOS sharpen, revealing a ν(P=O) peak at 158.5 meV, a $\nu_{a,s}$(O-P-O) band in the 120-150 meV region, and new peaks at 111, 93, 67 meV. This is consistent with the appearance of a new ER order as suggested by the diffraction data - the structure consists of mainly a random packing of corner-sharing PO_4 chains intervened by Na^+ ions.

Although it is difficult to compare the PDOS with Raman and infrared spectra for the aforementioned reasons as well as for the different water contents and modifier compositions in the samples reported by various authors, qualitatively, our neutron data agree well with those of previous optical studies.[34-42]

3.2. $Pb(PO_3)_2$ and $(PbO)_2P_2O_5$ glasses

Fig. 3 shows the observed generalized PDOS of lead metaphosphate glass, the crystalline and glassy lead pyrophosphates at 15 K. The PDOS of g-$Pb(PO_3)_2$ [or equivalently, g-$(PbO)_{50}(P_2O_5)_{50}$] resembles to that of the sodium metaphosphate (Fig. 2d). The O-P-O and P=O stretch vibrational energies of the lead metaphosphate glass are slightly lower, and the phonon density below ~30 meV is higher due to the heavier mass and larger neutron scattering cross section of Pb atoms. The PDOS of the crystalline and glassy lead pyrophosphate have similar shapes except the peaks of the glassy sample are broader. In the unit cell of c-$Pb_2P_2O_7$ there are four corner-sharing PO_4 dimers (P_2O_7 groups).[43] Therefore, as more Pb modifier is

added into the glass, the PO_4 chains in the metaphosphate are shortened, and eventually the structure of the pyrophosphate glass consists of mainly PO_4 dimers. The P=O stretch vibrations show diminishing intensities. This trend continues as it can be seen from the PDOS of crystalline compounds of orthophosphates. For example, in the case of $LuPO_4$, all the PO_4 units are disconnected and exhibit only two unique P-O bond distances. The PDOS shows two sharp peaks at about 128 and 135 meV corresponding to the ν_a(O-P-O) and ν_s(O-P-O) stretch vibrations, respectively, and a phonon gap develops in the 90-115 meV region.[44] Our conclusion on the structure and dynamics of the $(PbO)_y(P_2O_5)_{100-y}$ system is in good agreement with the results of previous studies.[7, 26, 45]

3.3 $(PbO)_{54.2}(Sc_2O_3)_{3.6}(P_2O_5)_{42.2}$ and $(PbO)_{56.2}$ $(P_2O_5)_{43.8}$ glasses

In order to investigate the structural modification induced by Sc atoms in the lead phosphate glass, we compare the diffraction data of the $(PbO)_{54.2}(Sc_2O_3)_{3.6}(P_2O_5)_{42.2}$ and $(PbO)_{56.2}$ $(P_2O_5)_{43.8}$ glasses. The observed static structure factors and the difference profile of the two glasses (seeFig. 4) show that the major difference occurs only at a low-Q region. In other words, the presence of the Sc atoms affects mainly the MR order structure. In order to minimize the Q-dependent effect of the resolution on the correlation functions, we express the results in terms of the total distribution function T(r) and the radial distribution function N(r) which are related to the G(r) of Eq. (1) by

$$T(r) = 4\pi r \rho_0 G(r) \ , \tag{2}$$

and

$$N(r) = 4\pi r^2 \rho_0 G(r) = rT(t) \ . \tag{3}$$

N(r)dr has a direct physical interpretation as the number of atoms lying within a range (r, r+dr) from any given atom. The area under a peak in N(r) is directly proportional to the coordination number of the atoms.

Fig. 5a shows the T(r) functions of lead phosphate glasses with and without Sc. They oscillate about a line with a slope given by the density of the glass. The peaks in T(r) represent the most probable (average) bond distances for various combinations of elements. The peak centered at 1.54 Å corresponds to the mean nearest P-O distance. The peak at 2.52 Å includes a major contribution of the nearest O-O correlation as well as the Pb-O correlation. The residual T(r) obtained by subtracting the Pb, P, and O contributions of the g-Pb-P-O data from the data of the g-Pb-Sc-P-O reveals the MR correlation of Sc and O around 2.0-2.1 Å. We fitted the T(r) profiles representing the appropriate P-O, Pb-O + O-O, and Sc-O for both glasses. The result of the fit for the g-Pb-Sc-P-O is show in Fig. 5b. The average bond distance and coordination number of P-O (1.54 ± 0.01 Å, 4.0 ± 0.1), Pb-O (2.52 Å, 5.2), and O-O (2.52 Å, 3.67) are the same for the two glasses. In the calculations of Pb-O and O-O correlations, we assumed an identical P-O and O-O bond distance which was determined by the position of the single peak at 2.52 Å. The N_{O-O} was first determined from the composition of the Pb-P-O glass[46] and the corresponding contribution in T(r) was evaluated. An N_{Pb-O} of 5.2 was then obtained by fitting the residual peak area. For this reason, we did not assign the uncertainties to these values. Finally, the average bond distance and coordination number of Sc-O in the Pb-Sc-P-O glass (2.105 ± 0.02 Å, 6.1 ± 0.3) were obtained. The coordination numbers for Pb-O and Sc-O are reasonable as they agree very well with those found in a $PbO{\bullet}P_2O_5$ glass by Hoppe *et al.*[47] and in c-Sc_2O_3 by Knop *et al.*[48] The PDOS of the Pb-Sc-P-O glass is given in Fig. 3d. It is

similar to the PDOS of the lead pyrophosphate glass but the features are better resolved by the HRMECS instrument.

4. Summary

We have applied the methods of neutron diffraction and inelastic scattering to investigate the structural changes of phosphate glasses induced by adding framework modifier cations. In both the ultra-to-metaphosphate $(Na_2O)_x(P_2O_5)_{100-x}$ and the meta-to-pyrophosphate $(PbO)_y(P_2O_5)_{100-y}$ glasses we observed the initial break-down of the cross-linking network structure and the modification of intermediate-range order in ultraphosphate compositions. We find evidence of the appearance of an extended-range order structure corresponding to the predominant chain-like and the dimer-like structures in the metaphosphate and pyrophosphate compositions, respectively. In addition, we determined quantitatively the short-range order and the spatial correlations of nearest atomic pairs in an optical glass of $(PbO)_{54.2}(Sc_2O_3)_{3.6}(P_2O_5)_{42.2}$.

Acknowledgment

We thank J. U. Otaigbe and M.-L. Saboungi for many helpful discussions. The assistance from K. Volin and L. I. Donley in the neutron experiments is gratefully acknowledged. Work performed at Argonne and Oak Ridge is supported by the U.S.DOE-BES under Contact Nos.W-31-109-ENG-38 and DE-AC05-96OR22464, respectively.

References

1. S. W. Martin, J. Am. Ceram. Soc. **74**, 1767 (1991).
2. H. Hosono, S. Kawamura, and Y. Abe, J. Mat. Sci. Lett. **4**, 244 (1985).
3. J. U. Otaigbe, B. C. Monahan, C. J. Quinn, and G. H. Beall, J. Rheology , (in press) (1997).
4. C. J. Quinn, P. D. Frayer, and G. H. Beall, in *Polymeric Materials Encyclopedia* (CRC Press, 1996), Vol. 4, p. 2766.
5. B. C. Sales, MRS Bull. , 32 (1987).
6. B. S. Sales and L. A. Boatner, J. Am. Ceram. Soc. **70**, 615 (1987).
7. B. C. Sales and L. A. Boatner, J. Non-Cryst. Solids **79**, 83 (1986).
8. R. C. Ropp, *Inorganic Polymeric Glasses* (Elsevier, Amsterdam, 1992).
9. J. A. Wilder, Jr., J. Non-Cryst. Solids **38&39**, 879 (1980).
10. S. W. Martin, Eur. J. Solid State Inorg. Chem. **28**, 163 (1991).
11. T. Minami, Y. Takuma, and M. Tanaka, J. Electrochem. Soc. **124**, 1659 (1977).
12. H. Hosono, K.-I. Kawamura, H. Kawazoe, N. Matsunami, and Y. Abe, J. Appl. Phys. **81**, 1296 (1997).
13. G. Guo and Y. Chen, J. Mat. Sci. Lett. **12**, 265 (1993).
14. J. A. Duffy and M. D. Ingram, J. Non-Cryst. Solids **21**, 373 (1976).
15. Y. Abe, R. Ebisawa, and A. Naruse, J. Am. Ceram. Soc. **59**, 453 (1976).
16. Y. Abe and H. Hosono, in *Inorganic phosphate materials*, edited by T. Kanazawa (Elsevier and Kodansha, New York, 1989), p. 247.
17. J. E. Marion and M. J. Weber, Eur. J. Solid State Inorg. Chem. **28**, 271 (1991).
18. K. A. Cerqua, S. D. Jacabs, and A. Lindquist, J. Non-Cryst. Solids **93**, 36 (1987).

19. Y. Abe, K. Kawashima, and S. Suzuki, J. Am. Ceram. Soc. **64**, 206 (1981).

20. N. H. Ray, *Inorganic Polymers* (Academic Press, New York, 1978).

21. B. Aitken and G. Beall, in *Structure and properties of ceramics*, edited by M. V. Swain (VCH, Weinheim, Germany, 1994), Vol. 11, p. 267.

22. L. L. Hench and Ö. Andersson, in *An introduction to bioceramics*, edited by L. L. Hench and J. Wilson (World Scientific, Singapore, 1993), p. 41.

23. W. Höland and W. Vogel, in *An introduction to bioceramics*, edited by L. L. Hench and J. Wilson (World Scientific, Singapore, 1993), p. 125.

24. A. Ravaglioli and A. Krajewski, *Bioceramics* (Chapman & Hall, London, 1992).

25. P. A. Tick, Phys. Chem. Glasses **25**, 149 (1984).

26. B. C. Sales, R. S. Ramsey, J. B. Bates, and L. A. Boatner, J. Non-Cryst. Solids **87**, 137 (1986).

27. K. Suzuya, D. L. Price, C.-K. Loong, and S. W. Martin, in *7th International Conference of the Non-crystalline Materials*, Sardegna, Italy, 1997).

28. B. C. Sales, M. M. Abraham, J. B. Bates, and L. A. Boatner, J. Non-Cryst. Solids **71**, 103 (1985).

29. C.-K. Loong, S. Ikeda, and J. M. Carpenter, Nucl. Instrum. Methods **A 260**, 381 (1987).

30. A. J. G. Ellison, R. K. Crawford, D. G. Montague, K. J. Volin, and D. L. Price, J. Neutron Res. **1**, 61 (1993).

31. K. Suzuki and M. Ueno, J. Phys. (Paris) **46**, C8 (1985).

32. U. Hoppe, G. Walter, D. Stachel, and A. C. Hannon, Z. Naturforschg. **51a**, 179 (1996).

33. S. C. Moss and D. L. Price, in *Physics of Disordered Materials*, edited by D. Adler, H. Fritzsche and S. R. Ovshinsky (Plenum, New York, 1985), p. 77.

34. R. K. Brow, D. R. Tallant, J. J. Hudgens, S. W. Martin, and A. D. Irwin, J. Non-Cryst. Solids **177**, 221 (1994).

35. S. W. Martin and C. A. Angell, J. Phys. Chem. **90**, 6736 (1986).

36. B. N. Nelson and G. J. Exarhos, J. Chem. Phys. **71**, 2739 (1979).

37. F. L. Galeener and J. C. Mikkelsen, Jr., Solid State Commun. **30**, 505 (1979).

38. S. Krimi, A. E. Jazouli, L. Rabardel, M. Couzi, I. Mansouri, and G. L. Flem, J. Solid State Chem. **102**, 400 (1993).

39. G. B. Rouse, Jr., P. J. Miller, and W. M. J. Risen, J. Non-Cryst. Solids **28**, 193 (1978).

40. K. Meyer, H. Hobert, A. Barz, and D.Stachel, Vibr. Spect. **6**, 323 (1994).

41. C. Garrigou-Lagrange, M. Ouchetto, and B. Elouadi, Canad. J. Chemistry **63**, 1436 (1985).

42. K. Meyer, A. Barz, and D. Stachel, J. Non-Cryst. Solids **191**, 71 (1995).

43. D. F. Mullica, H. O. Perkins, D. A. Grossie, L. A. Boatner, and B. C. Sales, J. Solid State Chem. **62**, 371 (1986).

44. J. C. Nipko, C.-K. Loong, M. Loewenhaupt, M. Braden, W. Reichart, and L. A. Boatner, Phys. Rev. , in press (1997).

45. B. C. Sales, R. S. Ramsey, J. B. Bates, and L. A. Boatner, Mat. Res. Soc. Symp. Proc. **81**, 455 (1986).

46. $N_{o\text{-}o} = 24/(5+z)$ where z is the molar ratio of PbO and P_2O_5 of the glass.

47. U. Hoppe, G. Walter, D. Stachel, and A. C. Hannon, Z. Naturforschg. **50a**, 684 (1995).

48. Knop, Canad. J. Chemistry **46**, 1446 (1968).

Figure captions

Figure 1. The static structure factors of g-$(Na_2O)_x(P_2O_5)_{100-x}$ of ultraphosphate ($x < 50$) and metaphosphate ($x = 50$) compositions. The downward pointing and upward pointing arrows label the small-Q diffraction peaks indicative of intermediate-range and extended-range order structure, respectively.

Figure 2. The generalized phonon densities of states of c-P_2O_5, g-P_2O_5, g-$(Na_2O)_{20}(P_2O_5)_{80}$, and g-$(Na_2O)_{50}(P_2O_5)_{50}$ obtained from LRMECS measurements with an incident neutron energy of 200 meV and sample temperature of 15 K.

Figure 3. The generalized phonon densities of states of g-$Pb(PO_3)_2$, c-$Pb_2P_2O_7$, g- c-$Pb_2P_2O_7$, and g-$(PbO)_{54.2}(Sc_2O_3)_{3.6}(P_2O_5)_{42.2}$ obtained from LRMECS (a-c) and HRMECS (d) measurements with an incident neutron energy of 200 meV and sample temperature of 15 K. The phonon features are better resolved by the HRMECS experiment.

Figure 4. The static structure factors of g-$(PbO)_{54.2}(Sc_2O_3)_{3.6}(P_2O_5)_{42.2}$ and g-$(PbO)_{56.2}$ $(P_2O_5)_{43.8}$. The difference-S(Q) is shown in the bottom of the graph.

Figure. 5. (a) The total distribution functions of g-$(PbO)_{54.2}(Sc_2O_3)_{3.6}(P_2O_5)_{42.2}$ and g-$(PbO)_{56.2}$ $(P_2O_5)_{43.8}$ and the residual T(r). (b) A fit of the T(r) of g-$(PbO)_{54.2}(Sc_2O_3)_{3.6}(P_2O_5)_{42.2}$ with Gaussian functions representing the correlations of nearest atomic pairs.

Table 1. Properties and technological applications of phosphate glasses

Properties	Outstanding features	Potential applications
Composition	Offer extremely wide range of compositions, possible to tailor the chain-like polymeric structure	Oriented metaphosphate glass fibers[2] Injection moldable glass-polymer melt blends[3, 4]
Preparation temperature	Low[a] Sn-Pb-F-P-O glass: $T_g \approx 100°C$[25] g-Pb-In-P-O glass: $T_m = 900°C$, $T_p = 800°$-$900°C$, $T_g = 436°$, $T_s = 459°C$[6]	Castable lenses and optical elements[5]
Chemical durability	Poor for ultraphosphate glasses, but can be strengthen drastically by incorporation of modifier oxides	Nuclear waste storage media[7, 8]
Thermal expansion	High. alkali-alkaline earth P-glasses: 10-20 X $10^{-6}/°C$[9]	Glass-to-metal seals
Electrical conductivity	Fast ionic conduction AgI-Ag_2O-P_2O_5 glasses: 10^{-3} - 10^{-2} $\Omega^{-1}cm^{-1}$[1, 11] Proton conduction H^+-implanted $Mg(PO_3)_2$ glass: d c conductivity 5 X 10^{-4} s cm^{-1}[12]	Solid electrolytes Fuel cell materials
Optical clarity	High index of refraction, 1.75 - 1.91 for Pb-In-P-O, Pb-Sc-P-O[6], and Pb-In-Al-P-O glasses[13] Moderately low dispersion	Optical applications
UV transparency	High-energy excitations of the bridging and nonbridging oxygen orbitals leads to superior UV-transparency[14, 16]	Wide-band optical fibers for communication
Stimulated emission	Narrow linewidths, high transition strengths, high refractive index and spectral homogeneity[17, 18] Photochromism and thermochromism[15, 19]	High average-power lasers Solar energy collectors light and heat sensitive colored glasses
Surface chemistry	Hydrolyzed, non-misting surface[20]	lenses and windows for marine applications

Nucleation and crystallization	Controlled formation of microstructure in glass-ceramics	Hydrogen-filled BPO_4 gas ceramic[21]
Biocompatibility and bioactivity	Capable of bonding to living bone by glass formation of a Ca-P rich surface film[22-24]	Bioglass Bioceramics

[a] Glass transition temperature (T_g), melting temperature (T_m), pouring temperature (T_p), softening temperature (T_s)

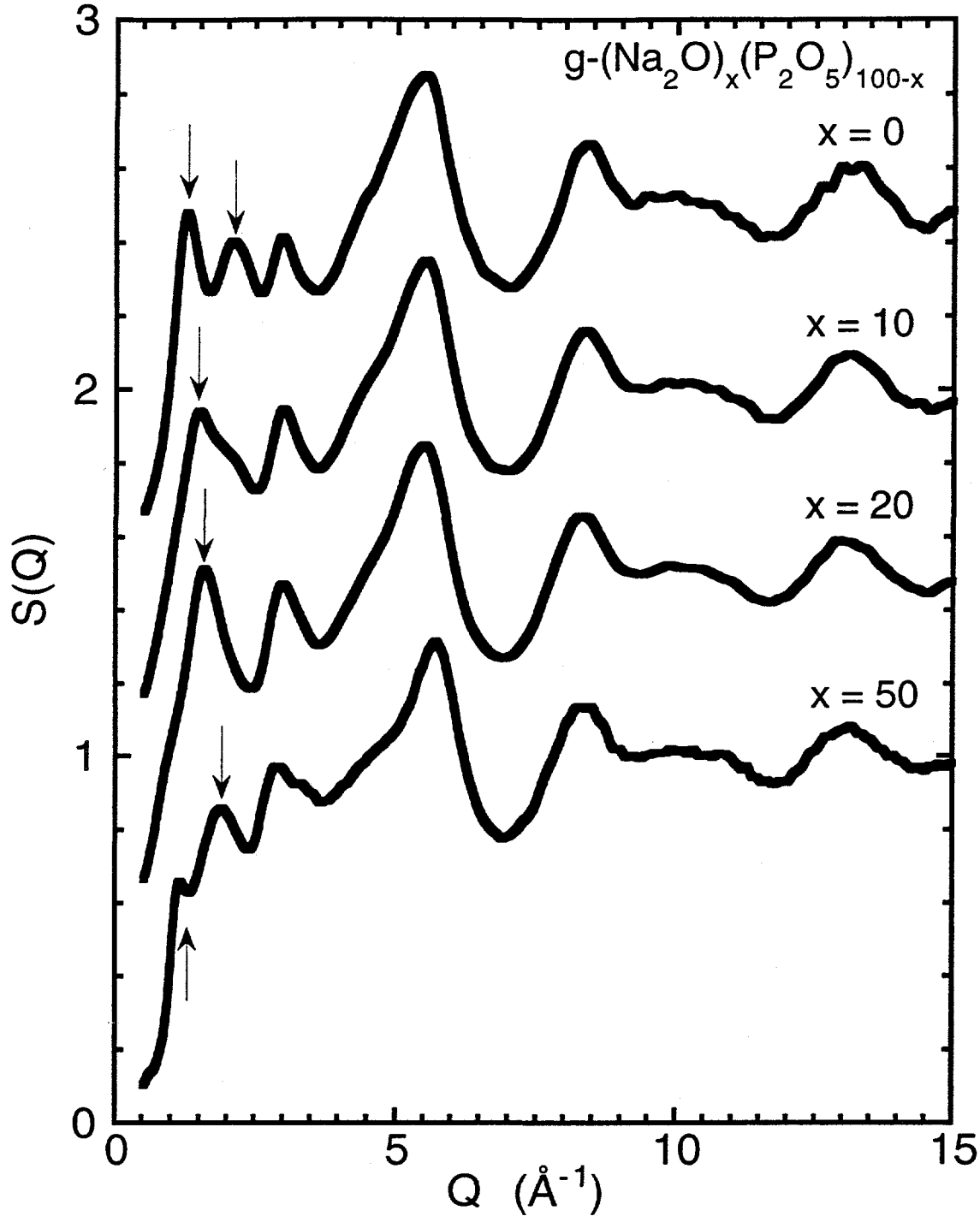

Fig. 1, Loong et al., "Structure and dynamics of phosphate glasses..."

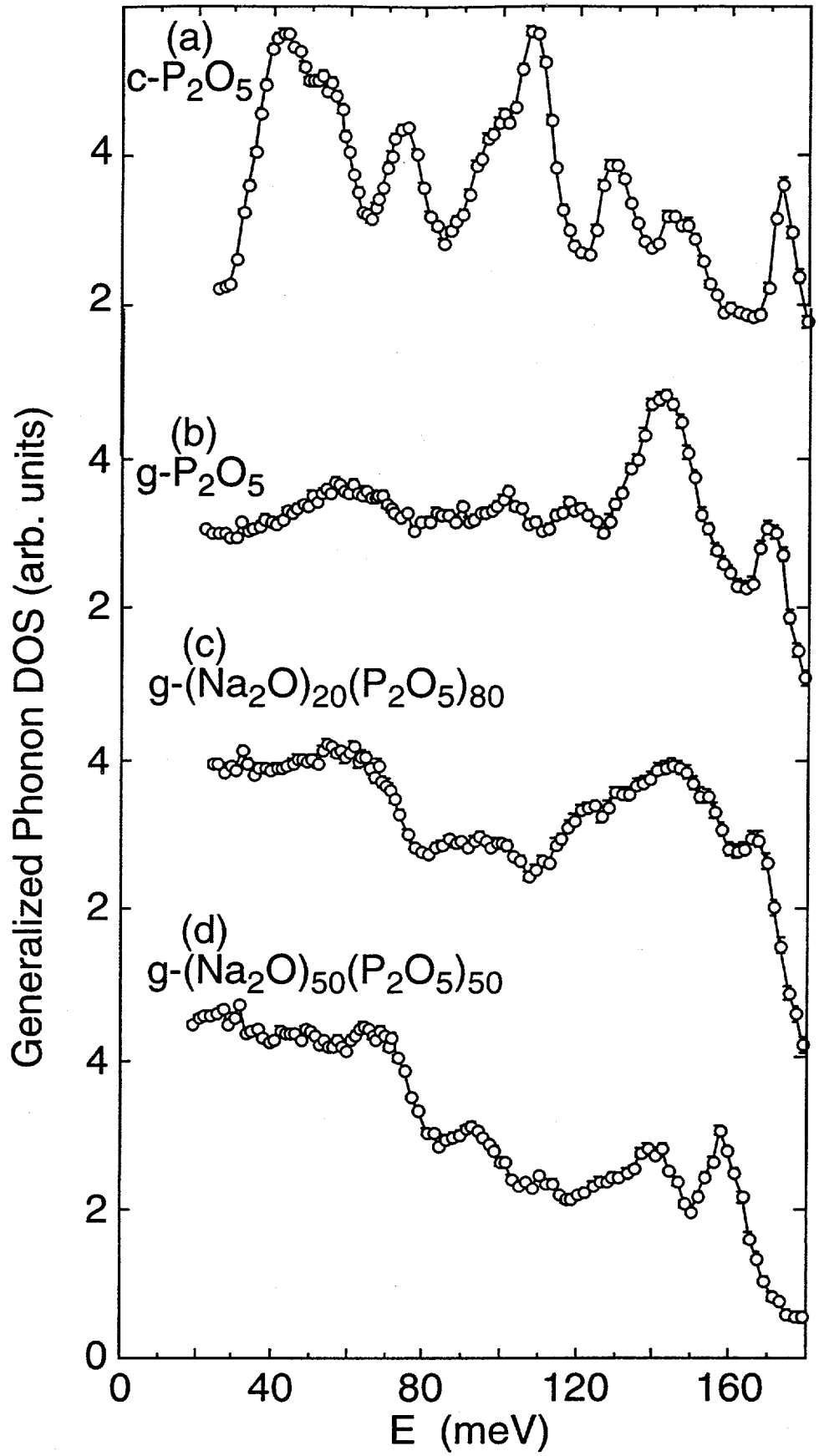

Fig. 2, Loong et al., "Structure and dynamics of phosphate glasses..."

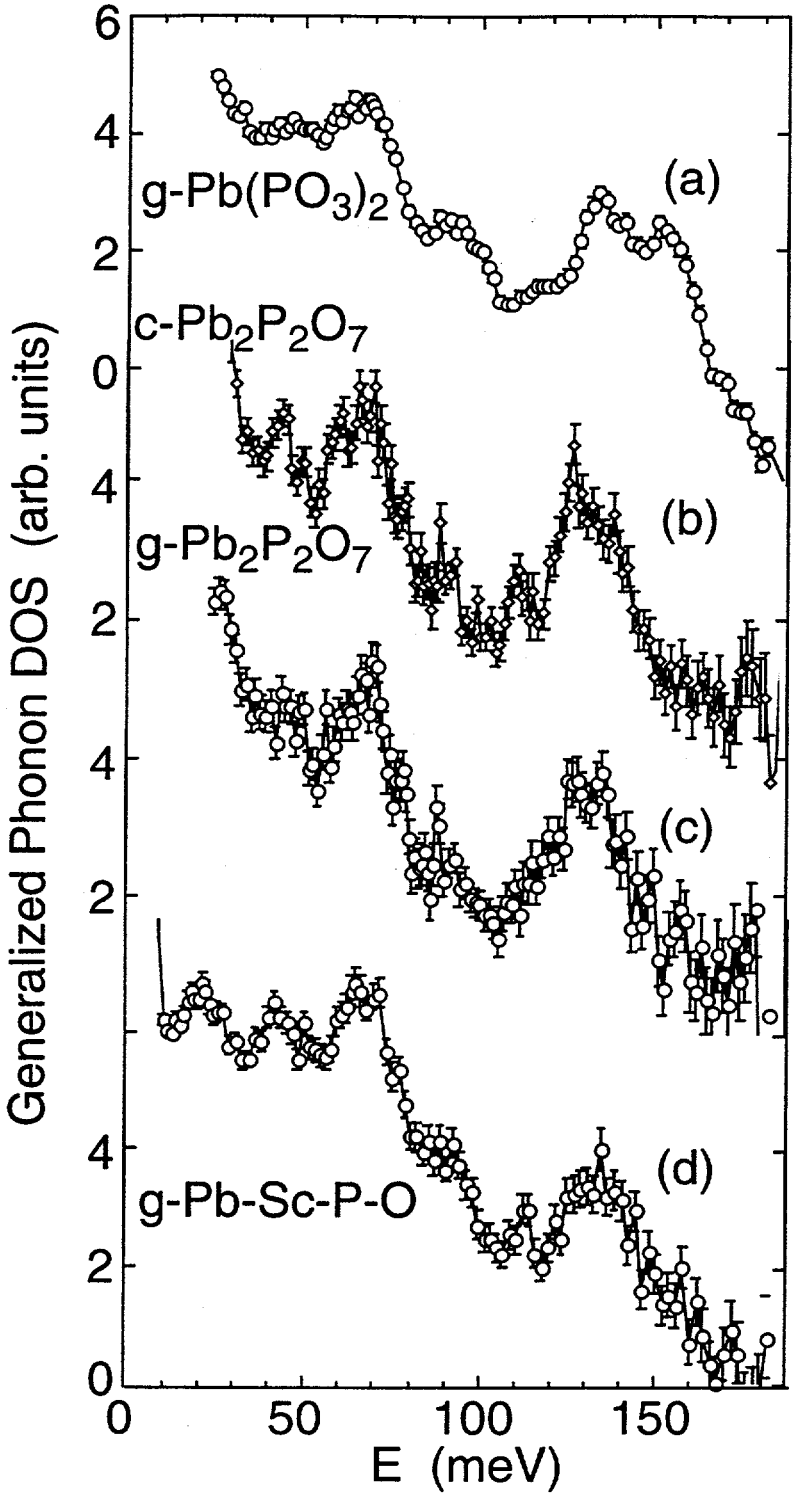

Fig. 3, Loong et al., "Structure and dynamics of phosphate glasses..."

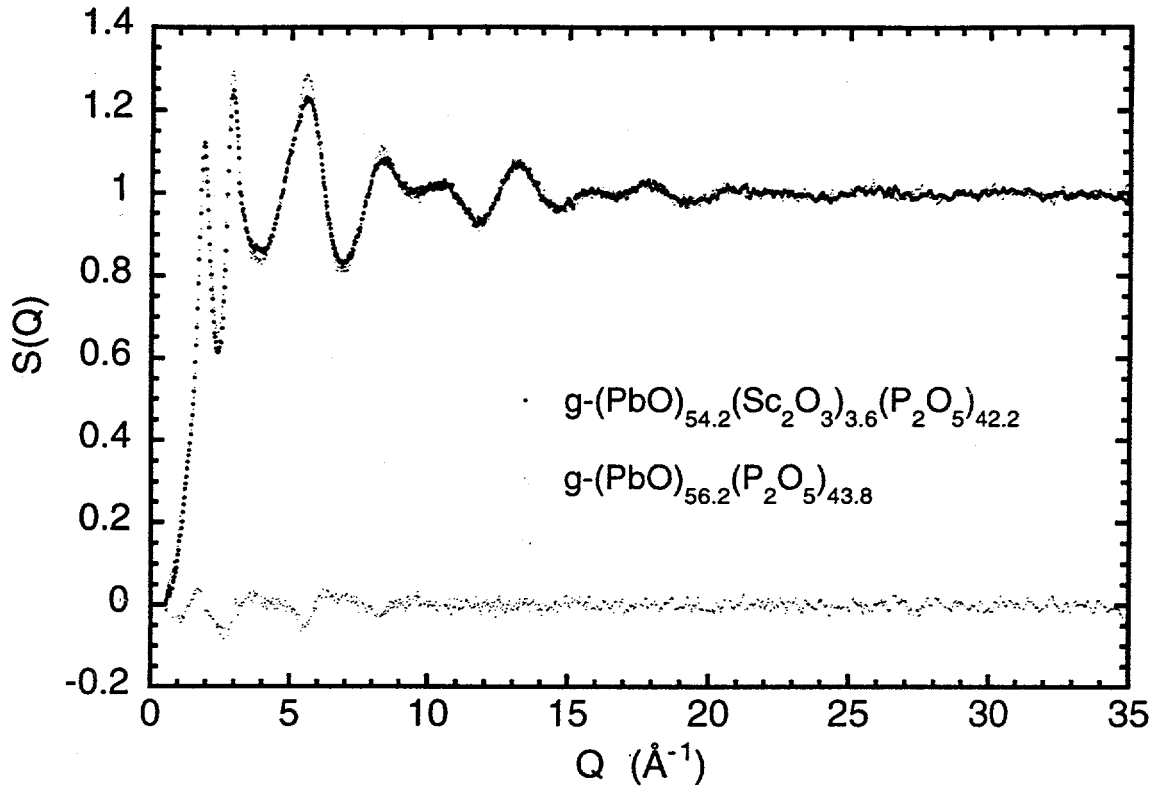

Fig. 4, Loong et al., "Structure and dynamics of phosphate glasses..."

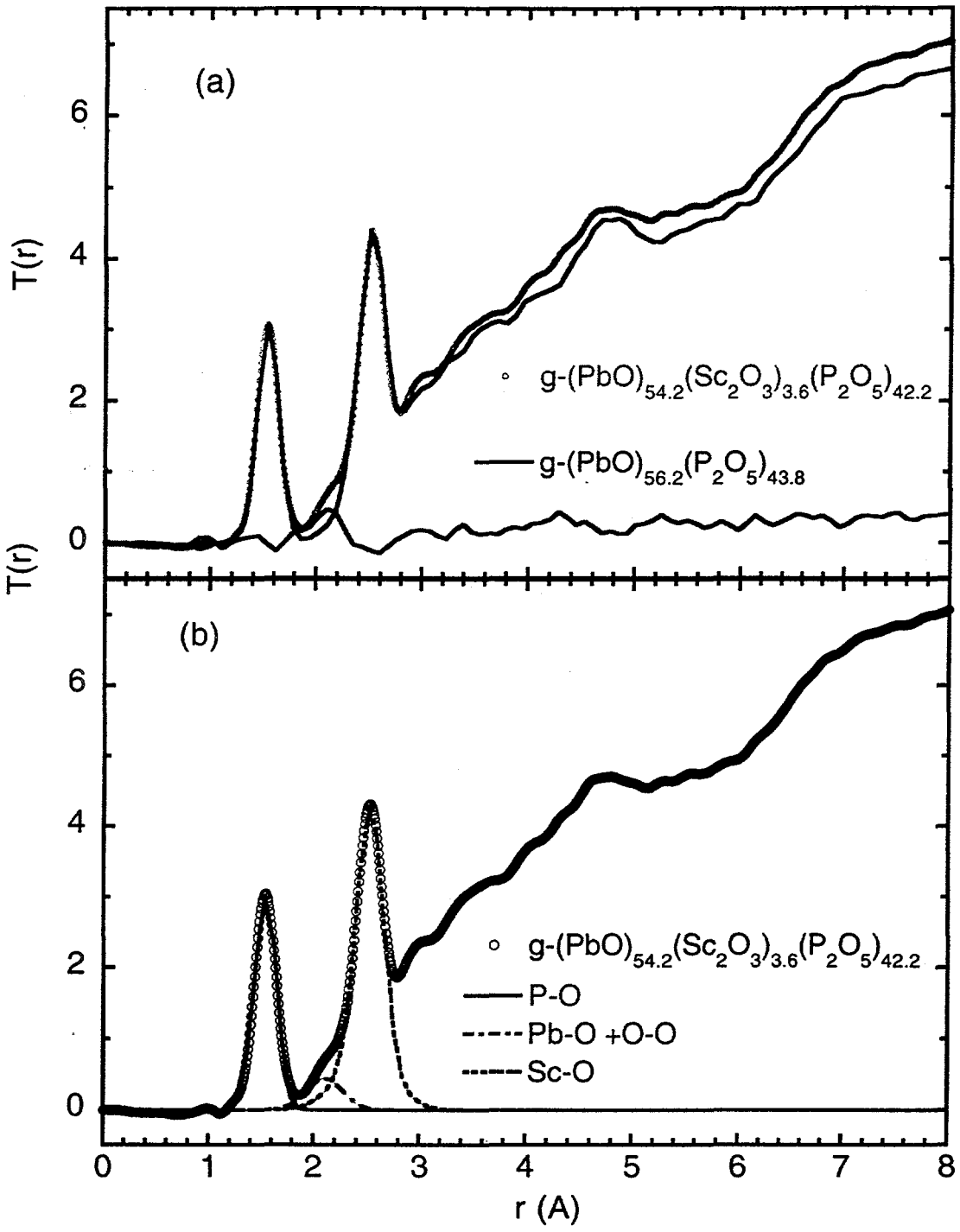

Fig. 5, Loong et al., "Structure and dynamics of phosphate glasses..."

Estimation of the length of this paper

a) Title, authors, affiliation and 122-word abstract		350 words
b) 5 figures, fitting a single column		750 words
c) 1 tables, double column, 30 lines		600 words
c) Manuscript text		2450 words
d) References (48)		720 words
	Total:	4870 words

For six printed pages: 4800 words